Molecular Pharmacology Fast Forward. Published on June 8, 2018 as DOI: 10.1124/mol.117.111443
This article has not been copyedited and formatted. The final version may differ from this version.

Title: Assessment of Substrate Dependent Ligand Interactions at the Organic Cation Transporter OCT2 Using Six Model Substrates

Authors:

Philip J. Sandoval, Kimberley M. Zorn, Alex M. Clark, Sean Ekins and Stephen H. Wright

Laboratories of Origin:

Department of Physiology, College of Medicine, University of Arizona, Tucson, AZ 85724: PJS, and SHW. Collaborations Pharmaceuticals, Inc., 840 Main Campus Drive, Lab 3510, Raleigh, NC 27606, USA., SE and KMZ. Molecular Materials Informatics, Inc., Montreal, Quebec, Canada., AMC.

Molecular Pharmacology Fast Forward. Published on June 8, 2018 as DOI: 10.1124/mol.117.111443
This article has not been copyedited and formatted. The final version may differ from this version.

Running Title Page

Running title: Substrate-Dependence of OCT2 Inhibition

Corresponding Author:

Stephen H. Wright, PhD

Department of Physiology, University of Arizona, Tucson, AZ 85724, Telephone: (520) 626-4253; Fascimile: (520)-626-2383.

E-mail; shwright@u.arizona.edu

Number of text pages:

Number of tables: 3
Number of figures: 8
Number of references: 39
Number of words in Abstract: 248
Number of words in Introduction: 755
Number of words in Discussion: 1487

Non-Standard Abbreviations:

ASP	4–4-dimethylaminostyryl-N-methylpyridinium
CHO	Chinese hamster ovary
Cu,max	maximum, unbound, drug concentration in plasma
DDI	drug-drug interaction
ECFP_6	Extended Connectivity Fingerprint
FCFP_6	Functional Connectivity Fingerprint
FDA	Food and Drug Administration
MATE	Multidrug And Toxin Extruder
MPP	1-methyl-4-phenylpyridinium
NBD-MTMA	N,N,N-trimethyl-2-[methyl(7-nitrobenzo[c][1,2,5]oxadiazol-4-yl)amino]ethanaminium
NCC	NIH Clinical Collection
NME	New Molecular Entity
OCT	Organic Cation Transporter
OC	organic cation
ROC	Reciever Operator Curve
RPT	renal proximal tubule
S.A.	Specific Activity

Molecular Pharmacology Fast Forward. Published on June 8, 2018 as DOI: 10.1124/mol.117.111443
This article has not been copyedited and formatted. The final version may differ from this version.

Abstract

The organic cation transporter OCT2 mediates the entry step for organic cation secretion by renal proximal tubule cells and is a site of unwanted drug-drug interactions (DDIs). But reliance on decision tree-based predictions of DDIs at OCT2 that depend on IC_{50} values can be suspect because they can be influenced by choice of transported substrate; for example, IC_{50}s for inhibition of metformin vs MPP transport can vary by 5 to 10-fold. However, it is not clear if substrate-dependence of ligand interaction is common among OCT2 substrates. To address this question we screened the inhibitory effectiveness of 20 μM concentrations of several hundred compounds against OCT2-mediated uptake of six structurally distinct substrates: MPP, metformin, NBD-MTMA, TEA, cimetidine, and ASP. Of these, MPP transport was least sensitive to inhibition. IC_{50} values for 20 structurally diverse compounds confirmed this profile, with IC_{50}s for MPP averaging 6-fold larger than for the other substrates. Bayesian machine learning models of ligand-induced inhibition displayed generally good statistics after cross validation and external testing. Applying our ASP model to a previously published large scale screening study for inhibition of OCT2-mediated ASP transport resulted in comparable statistics, with approximately 75% of 'active' inhibitors predicted correctly. The differential sensitivity of MPP transport to inhibition suggests that multiple ligands can interact simultaneously with OCT2 and supports the recommendation that MPP not be used as a test substrate for OCT2 screening. Instead, metformin appears to be a comparatively representative OCT2 substrate for both *in vitro* and *in vivo* (clinical) use.

Molecular Pharmacology Fast Forward. Published on June 8, 2018 as DOI: 10.1124/mol.117.111443
This article has not been copyedited and formatted. The final version may differ from this version.

Introduction

It is estimated that approximately 40% of all prescribed drugs are positively charged at physiological pH and that the kidney plays a significant role in the elimination of these 'organic cations' (OCs) from the body (Hagenbuch, 2010; Neuhoff et al., 2003). The proximal tubule is the site for the secretion of OCs via a two-step process that involves the transporters OCT2 and MATE1. It is widely accepted that in humans the initial step in OC secretion is mediated by the electrogenic uniporter OCT2, which relies on the inside negative potential of renal proximal tubule (RPT) cells to drive the net movement of OCs from the blood into the RPT (Budiman et al., 2000; Holohan and Ross, 1980); together, OCT2 and MATE help to define the pharmacokinetics of structurally diverse OCs that share these transporters as a common pathway for elimination. Competition for the limited number of transport sites in this shared pathway can result in altered pharmacokinetics of prescribed OCs, potentially resulting in adverse drug-drug interactions (DDIs) (Somogyi et al., 1987; Stage et al., 2015; Yin et al., 2016). Additionally, in drug development there is a significant cost in both time and money invested into assessing the DDI risk of new molecular entities (NMEs). Hence, prediction and prevention of DDIs through an understanding of the selectivity of OCT2/MATE would reduce costs in drug development in addition to improving healthcare.

OCT2 has been a particular focus of efforts to predict the likelihood that an NME will inhibit activity of the OC secretory process. The primary approach for assessing the selectivity of OCT2 uses cultured cells that express the transporter to determine the extent of inhibition of transport activity produced by each of a set of test agents (e.g., (Nies et al., 2011b)). But, whereas the set of inhibitory agents may be large and structurally diverse (e.g., (Kido et al., 2011)), transport activity is generally assessed by monitoring uptake of a single, presumably

Molecular Pharmacology Fast Forward. Published on June 8, 2018 as DOI: 10.1124/mol.117.111443
This article has not been copyedited and formatted. The final version may differ from this version.

representative, substrate. Interestingly, the pharmacophores generated by different groups to describe the molecular determinants of ligand interaction with OCT2, although qualitatively similar in their inclusion of several common structural characteristics (incl. hydrophobicity, hydrogen bonding features and positive charge), differ from one another with respect to the 3D placement of these elements (Liu et al., 2016; Nies et al., 2011a; Suhre et al., 2005; Xu et al., 2013; Zolk et al., 2009). This led to the suggestion that ligand interaction with OCT2 may be influenced by the choice of substrate used to assess transport activity (Belzer et al., 2013), an idea supported by the observation that IC_{50} values for inhibition of OCT2 activity produced by six commonly prescribed drugs were, on average, 9-10 fold greater when using MPP as a substrate than when using metformin as a substrate (Belzer et al., 2013; Zolk et al., 2009). Additionally, a follow up study that used 125 commonly prescribed drugs reported that OCT2-mediated metformin transport is significantly more sensitive to inhibition than is MPP transport (Hacker et al., 2015). These observations support the hypothesis that OCT2 has a complex binding surface where ligands may interact simultaneously at different sites (e.g., (Harper and Wright, 2012; Minuesa et al., 2009; Volk et al., 2003)). They also decrease confidence in the validity of recommendations to pursue (or not) clinical studies of DDIs produced by a suspected inhibitor that are based on inhibition of a single substrate (Giacomini et al., 2010). But, whereas differences in the inhibitory profiles for MPP and metformin have been reported repeatedly (Belzer et al., 2013; Hacker et al., 2015; Yin et al., 2016; Zolk et al., 2009), the extent of such differential substrate interactions with OCT2 is not clear. An assessment of the susceptibility of other OCT2 substrates to transport inhibition may provide insight into the mechanism of ligand interaction at OCT2 and clarify whether there is an 'ideal' substrate for characterizing drug affinity at OCT2, or if testing multiple substrates is the more prudent course.

Molecular Pharmacology Fast Forward. Published on June 8, 2018 as DOI: 10.1124/mol.117.111443
This article has not been copyedited and formatted. The final version may differ from this version.

Here we test the inhibitory effectiveness of 400+ compounds against the OCT2-mediated uptake of six structurally distinct substrates (metformin, cimetidine, TEA, MPP and the fluorescent probes ASP and NBD-MTMA). We also provide a quantitative comparison of our own OCT2 inhibition profiles to that reported by Kido et al. in their single substrate (ASP) screen of inhibition of OCT2 activity produced by 900 prescription drugs (Kido et al., 2011). These datasets were used for Bayesian machine learning analysis and development of predictive algorithms which we share herein, thereby allowing others to generate predictions of ligand interaction with OCT2 prior to *in vitro* testing.

Molecular Pharmacology Fast Forward. Published on June 8, 2018 as DOI: 10.1124/mol.117.111443
This article has not been copyedited and formatted. The final version may differ from this version.

Materials and Methods

Chemicals. [^{3}H]MPP (specific activity, (S.A., 80 Ci/mmol) was purchased from Perkin-Elmer; [^{3}H]cimetidine (S.A. 80 Ci/mmol) and [^{3}H]TEA (S.A. 54 Ci/mmol) were purchased from American Radiochemicals (St.Louis, MO); and [^{14}C]metformin (S.A. 90 mCi/mmol) was purchased from Moravek Biochemicals (Brea, CA). Unlabeled cimetidine and metformin were purchased from Sigma-Aldrich Co. (St. Louis, MO) and AK Scientific, Inc. (Union City, CA), respectively. The fluorescent compound, 4-(4-(dimethylamino)styryl)-*N*-methylpyridinium (ASP), was purchased from Invitrogen (Carlsbad, CA); the fluorescent compound N,N,N-trimethyl-2-methyl (7-nitrobenzo c 1,2,5 oxadiazol-4-yl) amino ethanaminium iodide (NBD-MTMA) (Aavula et al., 2006) (purity >97%) and the non-radioactively labeled MPP (purity >99.5%) were synthesized by the Department of Chemistry and Biochemistry, University of Arizona. Ham's F12 Kaighn's modified medium, and Dulbecco's modified Eagle medium were obtained from Sigma-Aldrich Co. The National Institutes of Health Clinical Collection (NCC), a plated array of approximately 900 small molecules that have a history of use in human clinical trials, was acquired from Evotec (San Francisco, CA). Other reagents were of analytical grade and were commercially obtained.

Drug Screening. Compounds from the NCC, distributed in 80 wells of 96 well plates (100 nmol per well in 10 μl of DMSO), were screened for their inhibitory effectiveness against the transport activity of six model substrates of OCT2. A total of 480 compounds were used for MPP, TEA, NBD-MTMA, and metformin; 400 compounds were used for cimetidine and ASP. Each compound was diluted to a concentration of 20 μM, pH 7.4, to a final concentration of 2% dimethylsulfoxide (DMSO) using a VIAFLO multichannel electronic pipet (Integra Biosciences, Hudson, NH) (Martinez-Guerrero et al., 2016).

Molecular Pharmacology Fast Forward. Published on June 8, 2018 as DOI: 10.1124/mol.117.111443
This article has not been copyedited and formatted. The final version may differ from this version.

Cell Culture. Chinese Hamster Ovary cells with a single integrated Flp-in recombination site were obtained from Invitrogen (Carlsbad, CA). Methods for generation of cell lines that stably express hOCT2 were described previously (Pelis et al., 2007). Cells were passed every 3-4 days and maintained at 37^{o}C in a humidified environment with 5% CO_2. Expression of hOCT2 in cells was maintained through hygromycin (purchased from Invitrogen, Carlsbad, CA, 200 μg/mL) selective pressure. When seeded into 96-well plates (Greiner; VWR Intl., Arlington Heights, IL) for transport assays, these cells were grown to confluence in antibiotic-free media.

Transport Experiments. Cells were seeded in 96 well plates with 200 μL of cell media containing 550,000 cells/mL or 275,000 cells/mL, and experiments were typically performed 24 or 48 hours later, respectively. To begin an experiment, media was aspirated and the wells were washed for three cycles with 300 μL of room temperature Waymouth Buffer (WB; 135 mM NaCl, 13 mM HEPES, 2.5 mM $CaCl_2 \cdot 2H_2O$, 1.2 mM $MgCl_2$, 0.8 mM $MgSO_4 \cdot 7H_2O$, 5 mM KCl, and 28 mM D-glucose; pH 7.4) using an automatic fluid aspirator/dispenser (Model 406, BioTek, Winooski, VT). Transport was then initiated by the addition of 60 μL of WB containing a radiolabeled or fluorescent substrate and other compounds as needed. For time-course experiments using ASP as a substrate, transport buffer was added using the automatic fluid aspirator/dispenser and for all other experiments transport buffer was added using the VIAFLO 96 well multichannel pipet. After selected time intervals, transport was terminated by rinsing with three cycles of cold WB (300 μL) or, for the measurement of OCT2-mediated ASP uptake, with a continuous rinse of 900 μL cold WB. For radiolabeled substrates uptake was quantified by adding 200 μL of scintillation cocktail per well and sealing the plates (Topseal-A, Perkin Elmer). After allowing the plates to sit for at least two hours, radioactivity was determined in a twelve channel multiwell scintillation counter (Wallac Trilux 1450 Microbeta, Perkin-Elmer).

Molecular Pharmacology Fast Forward. Published on June 8, 2018 as DOI: 10.1124/mol.117.111443
This article has not been copyedited and formatted. The final version may differ from this version.

Uptake of fluorescent substrates was assessed by adding 60 µL DMSO (for NBD-MTMA) or 100 µL of 1 mM sodium dodecyl sulfate (for ASP) and, after sitting for at least two hours, fluorescence was measured using an ClarioStar microplate reader (BMG Labtech, Ortenberg, Germany) with emission and excitation filters set to 490 nm and 540 nm for NBD-MTMA, or to 460 nm and 575 nm for ASP.

Transport Data Analysis – Kinetic parameters were based on estimates of the initial rate of uptake derived from either 30 sec (radiolabeled substrates) or 2 min (fluorescent substrates) determinations of net accumulation in CHO cells that stably expressed OCT2. For all six substrates the kinetics of uptake reflected the sum of two processes, (i) OCT2-mediated uptake that was described by Michaelis-Menten kinetics; and (ii) a non-saturable, first order component that was dominated by extracellular substrate left after the rapid rinsing procedure. Although the first order component was evident in parallel determinations of transport in wild type (non-OCT2 expressing) CHO cells (see Supplemental Figure 1; i.e, Fig. S1), we found that subtracting WT accumulation from total accumulation measured in OCT2 expressing cells frequently introduced errors into kinetic analyses, particularly at the high end of substrate concentration employed for some substrates (e.g., metformin). These errors reflected modest differences in the efficiency of rinsing extracellular substrate from the OCT2 and WT CHO cell lines, evident in differences in retention of an extracellular space marker following rinsing (data not shown). Consequently, kinetic parameters were determined from total uptake (mediated plus non-saturable) using the following relationship:

$$J = \frac{J_{max}[S]}{K_{tapp}+[S]} + K_{fo}[S] \qquad \text{eq. 1}$$

where J is the rate of mediated uptake from a substrate concentration of [S], J_{max} is the maximal rate of mediated substrate uptake; K_{tapp} is the apparent Michaelis constant, *i.e.*, the substrate

Molecular Pharmacology Fast Forward. Published on June 8, 2018 as DOI: 10.1124/mol.117.111443
This article has not been copyedited and formatted. The final version may differ from this version.

concentration in the bulk medium that resulted in half maximal mediated uptake; and K_{fo} is a first order rate constant describing the non-saturable (non-mediated) component of total net substrate accumulation. Rates of transport were expressed in moles per min, normalized to surface area of the confluent monolayer. For the purpose of comparison to rates reported in studies that normalize transport to cell protein, we find the factor of 0.035 mg cell protein cm^{-2} to be reasonably accurate (Schomig et al., 2006).

For screening the influence of test inhibitors on OCT2 activity, it proved adequate to determine mediated uptake by subtracting accumulation in WT CHO cells from total uptake (30 sec or 2 min, for radiolabeled or fluorescent substrates, respectively) in OCT2-expressing cells, measured in the presence and absence of test inhibitor. Resulting OCT2-mediated transport was expressed relative to that determined in absence of inhibitor (i.e., % of control uptake). In addition, for some compounds, the concentration of inhibitor that reduced mediated transport by 50% (IC_{50}) was determined by measuring the rate of OCT2-mediated substrate transport as a function of increasing inhibitor concentration, as described by:

$$J^* = \frac{J_{app}[S^*]}{IC_{50} + [I]} \qquad \text{eq. 2}$$

where J^* is the rate of OCT2-mediated transport of labeled substrate from a concentration of substrate equal to $[S^*]$ (which was selected to be at least 3-times less than the K_{tapp} for transport of that substrate), IC_{50} is the concentration of inhibitor that reduces mediated (i.e., blockable) substrate transport by 50%, and J_{app} is a constant that includes the maximal rate of substrate transport times the ratio of the inhibitor IC_{50} and the K_{tapp} for transport of the labeled substrate (Groves et al., 1994).

Half-maximum inhibitory concentrations were also predicted ($IC_{50\text{-pred}}$) from the screening inhibition measurements using the approach described by Kido (Kido et al., 2011):

Molecular Pharmacology Fast Forward. Published on June 8, 2018 as DOI: 10.1124/mol.117.111443
This article has not been copyedited and formatted. The final version may differ from this version.

$$J = J_0/[1 + (I/IC_{50\text{-pred}})] \quad \text{eq. 2}$$

where J and J_0 represent OCT2-dependent transport activity determined in the presence and absence of inhibitor, respectively, and I is the fixed inhibitor concentration (in this case, 20 μM). This approach gives reasonable inhibitor affinity estimates when the screening concentration is within the linear part of the IC_{50} curve, i.e., approximately 10 - 90% inhibition (Gao et al., 2002; Hu et al., 2016; Kido et al., 2011); in the present study this corresponded to IC_{50} values between 2 and 180 μM.

Results are presented as means ±SE. Unless otherwise noted, statistical analyses were performed using a two-tailed paired Student's t-test. Curve-fitting used algorithms in Prism 6.07 (GraphPad Software Inc, San Diego, CA).

Computational Modeling: We generated and validated Laplacian-corrected naive Bayesian classifier models using Discovery Studio version 4.1 (Biovia, San Diego, CA). Values of the AlogP; molecular weight; number of rotatable bonds, rings, aromatic rings, hydrogen bond acceptors, and hydrogen bond donors; molecular fractional polar surface area; and molecular function class fingerprints of maximum diameter 6 (FCFP_6) were used as the molecular descriptors. Compounds that reduced transport to less than 50% of control were classed as actives and everything else was classed as inactive. Computational models were validated using leave-one-out (LOO) cross validation, in which each sample was left out one at a time. A model was built using the remaining samples, and that model was used to predict the left-out sample. Each model was internally validated, receiver operator characteristic curve (ROC) plots were generated, and the cross-validated ROC's 'area under the curve' was calculated. Then, five-fold cross validation (i.e. leave out 20% of the data set, and repeat five times) was also performed.

Sixteen Bayesian models were built with the extended connectivity fingerprint 6 (ECFP6) descriptor only, using Assay Central (Collaborations Pharmaceuticals, Inc. Raleigh, NC) (Clark et al., 2015; Clark and Ekins, 2015), consisting of either training data only or combined with testing data for each probe mentioned previously. Chemical structures were examined for valence errors, anionic charges were neutralized, salts were removed, and certain molecules were omitted such as mixtures (e.g. dimenhydrinate) or non-drug like compounds (e.g. zinc-chloride) prior to building a respective model. Structures were also checked for accuracy against four common, reliable resources: CompTox (https://comptox.epa.gov/dashboard), ChemSpider (http://www.chemspider.com/), Merck Index (https://www.rsc.org/merck-index), Pubchem (https://pubchem.ncbi.nlm.nih.gov/); when there was not agreement across these resources, consistency was ensured across similar structures by removing any conflicting stereochemistry. The same threshold was used (50% inhibition or greater) as well as the same method of five-fold cross validation and ROC calculation. Testing datasets consisting of 80 compounds were collated to measure the predictive capability of training data and generate statistics.

Molecular Pharmacology Fast Forward. Published on June 8, 2018 as DOI: 10.1124/mol.117.111443
This article has not been copyedited and formatted. The final version may differ from this version.

Results

Kinetic Characterization of OCT2 Test Substrates. OCT2-mediated transport activity was determined using six substrates: metformin, cimetidine, MPP, TEA, ASP, and NBD-MTMA. These compounds were chosen because they are (i) known substrates of OCT2, (ii) structurally diverse (Fig. 1 and Supplemental Table S1), and (iii), in the case of metformin and cimetidine, clinically relevant (Nies et al., 2011b). Two minute time courses showing OCT2-mediated net uptake of all six substrates are shown in Figure 1. The time courses for MPP, TEA, metformin, and cimetidine were curvilinear and adequately described by one-phase association (first-order exponential rise to steady state; Prism 5, GraphPad, San Diego); NBD-MTMA and ASP uptakes were described by simple linear regression (Fig. 1). Subsequent kinetic analyses used 30 second uptakes for the radiolabeled substrates metformin, cimetidine, MPP, and TEA, resulting in 5-25% underestimates of the initial rates of transport (as predicted from the slopes at time zero of the one phase association curves; Fig. S1). The initial rates of transport of the fluorescent substrates NBD-MTMA and ASP transport were based on two minute uptakes, which were within the apparent linear phase of transport.

Figure 2 shows the kinetic profiles for OCT2-mediated transport of the test substrates and highlights another basis for their inclusion in this study, namely, the wide range of their kinetic parameters. The kinetic values determined in 2 to 8 separate experiments for each substrate are summarized in Table 1. J_{max} values ranged from 17 pmol cm^{-2} min^{-1} (for MPP) to 656 pmol cm^{-2} min^{-1} (for metformin), and K_{tapp} values ranged from 5 μM (for MPP) to 285 μM (for metformin); the kinetic parameters for all substrates were within the range reported previously by us and others (Belzer et al., 2013; Harper and Wright, 2012; Nies et al., 2011b; Severance et al., 2017; Suhre et al., 2005).

Molecular Pharmacology Fast Forward. Published on June 8, 2018 as DOI: 10.1124/mol.117.111443
This article has not been copyedited and formatted. The final version may differ from this version.

Screening of Inhibition of OCT2-Mediated Transport. We initially determined the effect of between 320 and 400 (depending on the substrate) compounds from the NCC on transport of each of the six test substrates. These compounds were used as the 'training set' for the development of Bayesian models discussed later in this report. In order to validate these models a test set of an additional 80 compounds was used against the OCT2 mediated transport of these substrates, resulting in a total of 400 to 480 tested compounds. These 480 compounds are structurally diverse and included molecules that are predicted to carry a net positive (~31.2%), negative (~19.4%), or neutral (~49.4%) charge at physiological pH (see Table S2 in the supplement). Figure 3A shows the effect of a 20 μM concentration of each of 480 compounds (Table S3) on OCT2-mediated transport of 12 μM [^{14}C]metformin. Presented in rank order of increasing inhibitory potency, 87 of these compounds (18%) blocked metformin transport by at least 50%. These same compounds were also tested against transport of [^{3}H]MPP (15 nM), but only 43 (9%) blocked transport by at least 50% (Fig. 3B). The inset of Fig. 3B shows the profile of inhibition of MPP transport with the test agents rank ordered according to their inhibition of metformin; although the rank order of effectiveness differed somewhat, the overall profile of inhibition was similar to that observed for metformin. The difference in apparent sensitivity to inhibition of OCT2 activity between transport of metformin and MPP was particularly evident when the results for individual inhibitors of each substrate were compared in a pairwise fashion (Fig. 3C). Focusing on the 225 compounds that inhibited metformin transport by at least 10% (indicative of IC_{50} values < 200 μM), 89% of these compounds were more effective inhibitors of metformin transport than of MPP transport. Overall (by paired t-test), these compounds were more effective inhibitors of metformin transport than of MPP transport ($P < 0.05$), and on average reduced metformin transport by about 34% more than they did MPP transport.

Molecular Pharmacology Fast Forward. Published on June 8, 2018 as DOI: 10.1124/mol.117.111443
This article has not been copyedited and formatted. The final version may differ from this version.

Figure 4 shows the rank ordered inhibition profiles for OCT2-mediated transport of cimetidine, TEA, NBD-MTMA, and ASP (with insets showing profiles that used the metformin rank order) (Table S3). These profiles were qualitatively similar to those observed for metformin and MPP, with the 50% inhibition standard produced by 74 (15%), 90 (19%), 81 (20%), or 92 (23%) compounds, against the transport of TEA, NBD-MTMA, cimetidine or ASP, respectively. Figure 5 shows the pairwise comparisons of inhibition produced by these compounds versus inhibition of metformin (Fig. 5A, C, E, G) and MPP (Fig. 5B, D, F, H); MPP was consistently the least sensitive to inhibition when compared to the inhibitory profiles of these other substrates. Pairwise comparisons of these other substrates against metformin revealed smaller, albeit statistically significant, differences between the inhibitory profiles of TEA, NBD-MTMA, and ASP. Metformin transport was approximately 3% more sensitive to inhibition than TEA and NBD-MTMA and 7% less sensitive to inhibition than ASP ($P < 0.0001$ for TEA, $P < 0.001$ for NBD-MTMA, $P < 0.0126$ for ASP). With a 0.6% difference between the average observed inhibition, the inhibitory profile for cimetidine was not significantly different from the inhibitory profile of metformin ($P = 0.45$).

The systematic influence of substrate identity on inhibition of OCT2 activity was examined in more detail by determining IC_{50} values for a subset of the NCC test compounds. Figure 6A shows the effect of increasing concentrations of a representative test inhibitor (irinotecan) on the OCT2-mediated transport of MPP and metformin. Consistent with the general observation evident from the single concentration screening data presented in Figure 3, the IC_{50} for irinotecan inhibition of MPP transport was 4-fold larger than that for inhibition of metformin transport (13.8 μM vs. 3.4 μM; Table 2). Figure 6B shows the composite IC_{50} data for irinotecan inhibition of transport of 3 additional substrates, with IC_{50} values of: TEA (4.7

μM), NBD-MTMA (4.0 μM) and ASP (3.0 μM). The IC_{50} for inhibition of MPP transport was consistently 3- to 4-fold greater than those for the other test substrates (Table 2; Fig. S2). Figure 7A shows the pairwise comparison of IC_{50} values for inhibition of MPP and metformin transport for 20 compounds selected from the screening set. IC_{50} values for inhibition of MPP transport were, on average, 5.7-fold greater (570%) than those for inhibition of metformin transport. It is relevant to note that the IC_{50} values for these compounds calculated from the screening data, using control uptake (100%) and the single point reflecting transport measured in the presence of 20 μM inhibitor, correlated closely with the measured IC_{50} values. Figure 7B and 7C show pairwise comparisons of 'measured vs. predicted' IC_{50} values for MPP and metformin, respectively; the predicted IC_{50}s differed from the measured values by less than 40%. This degree of concordance suggested that a comparison of the predicted IC_{50} values from the screening data would permit an expanded view of the relative inhibitory profiles for OCT2-mediated transport of MPP and metformin that reflected a broader range of substrate structure than that afforded by the subset of compounds included in Figure 7A, while also providing a pharmacological context afforded by IC_{50} values (rather than '% of control'). Figure 7D shows the pairwise comparisons of predicted IC_{50} values for inhibition of metformin transport against those for MPP transport (estimated from percent control values between 10% and 90%, a total of 162 compounds). Of these predicted IC_{50} values, 29% differed by more than three-fold (designated by the dashed lines in Fig. 7D; Table S3).

Modeling OCT2 selectivity. Eliminating the inhibitory profiles for MPP and ASP, as the least and most sensitive substrates to inhibition of transport activity, respectively, we generated a 'Consensus' profile based on the average of inhibition produced by each inhibitor against transport of metformin, TEA, cimetidine and NBD-MTMA. These data were used to calculate

Molecular Pharmacology Fast Forward. Published on June 8, 2018 as DOI: 10.1124/mol.117.111443
This article has not been copyedited and formatted. The final version may differ from this version.

predicted IC_{50} values that reflected average inhibitory interactions with OCT2, ignoring those compounds that inhibited less than 10% of transport activity (i.e., predicted IC_{50} values of > 180 μM). Employing methods described elsewhere (Martinez-Guerrero et al., 2016), these data were then used in an attempt to generate a pharmacophore highlighting the common structural features correlated with ligand interaction with OCT2. These efforts, however, failed to converge on a unique pharmacophore using Discovery Studio.

We then applied machine learning methods to develop Bayesian models using results of the 400 (metformin, MPP, TEA, NBD-MTMA) or 320 (cimetidine, ASP) drugs in the initial 'training set' screening (Table S3). Using 50% reduction of OCT2-mediated uptake as the cutoff for 'active' inhibitors (the same criterion used by Kido et al. in their screening of inhibition of OCT2-mediated ASP transport (Kido et al., 2011)), the resulting Discovery Studio models had areas under the receiver operator curve (ROC; using 5-fold cross validation) of between 0.768 (ASP) and 0.806 (NBD-MTMA) (Table 3). These models adequately described the training set with 68% (MPP) to 86% (metformin) concordance (the sum of correctly predicted inhibitors and non-inhibitors divided by the total number of test compounds) for all the test substrates (Table 3). The consensus profile of OCT2 inhibition (reflecting average inhibition of metformin, TEA, cimetidine and NBD-MTMA transport for each inhibitor in the training set) resulted in an ROC of 0.798 and a concordance of 87% (Fig S3; Table 3). Use of the FCFP_6 descriptors with Discovery Studio Bayesian models allowed the identification of molecular features that favored inhibition (incl. basic nitrogens, tertiary amines, multiple aromatic rings; Fig. S4A) as well as features that did not promote inhibition (incl. acid features, hydroxyl and carbonyl groups; Fig. S4B). These models were validated by determining inhibition of OCT2-mediated transport of each substrate produced by a test set of 80 novel compounds from the NCC. The resulting ROC

Molecular Pharmacology Fast Forward. Published on June 8, 2018 as DOI: 10.1124/mol.117.111443
This article has not been copyedited and formatted. The final version may differ from this version.

values ranged from 0.806 (cimetidine) to 0.848 (metformin) with concordances from 68% (NBD-MTMA) to 81% (ASP) (except for the MPP model, which had an ROC for the test set of 0.619 and a concordance of 52%) (Table 3).

In addition to using Discovery Studio we also used Assay Central to generate 16 models which used Bayesian algorithm and ECFP6 fingerprints alone (Table S4). These models were built, cross validated and externally validated as described for the other models. Training model ROCs were between 0.775 (ASP training model) and 0.819 (metformin training model) with concordances of 75% and 80%, respectively. The consensus training model had an ROC of 0.810 and concordance of 68%; the consensus testing set had an ROC of 0.797 and concordance of 39%. These values were within 3% of those generated by Discovery Studio.

We took the opportunity to compare the profile for inhibition of ASP transport we observed with that reported by Kido and colleagues in their assessment of inhibition of OCT2-mediated ASP transport produced by a 20 μM concentration of each member of a 900-compound drug library (Kido et al., 2011). The Kido library contained 656 compounds that were not included in the set of compounds we screened against ASP transport and 595 compounds that were not contained in the set of compounds in our Consensus library of OCT2 inhibitors. Using the unique Kido compounds as a test set against our ASP and OCT2 Consensus models with Assay Central analysis resulted in ROCs of 0.768 and 0.756, and concordances of 79% and 73%, respectively (Fig. S5). In other words, the Bayesian models generated from the present results in Assay Central correctly identified ~75% of the inhibitors and non-inhibitors determined in a previously published, independent study of OCT2 selectivity.

The Assay Central Bayesian machine learning models are included in the Supplemental Data. A major part of the value proposition of Assay Central is to have a growing number of

Molecular Pharmacology Fast Forward. Published on June 8, 2018 as DOI: 10.1124/mol.117.111443
This article has not been copyedited and formatted. The final version may differ from this version.

target models, as well as models for ADME off-targets, in the same place and of similarly high quality, using the same data formats and technologies. We suggest that access to models like these will assist academia and industry to maximize the utility of data concerning OCT2 and other transporters that is accumulating in the literature.

Molecular Pharmacology Fast Forward. Published on June 8, 2018 as DOI: 10.1124/mol.117.111443
This article has not been copyedited and formatted. The final version may differ from this version.

Discussion

OCT2 is a target for clinically significant drug-drug interactions (DDIs) and, as such, has been the focus of studies investigating ligand specificity and decision tree-based assays to determine the likelihood that novel therapeutic compounds will act as perpetrators of unwanted interactions (Giacomini et al., 2010; Hillgren et al., 2013). The International Transport Consortium initially suggested that either MPP or metformin be used as OCT2 probe substrates to assess the DDI potential of new molecular entities (NMEs) (Giacomini et al., 2010), a recommendation subsequently supported by the FDA in their 2012 draft guidance to industry (U.S.Food and Drug, 2012). Ensuing evidence that substrate identity can exert a marked influence on inhibition of transport activity (Belzer et al., 2013; Yin et al., 2016) challenged that suggestion by showing that the decision-tree criterion of C_{max}/IC_{50}, i.e., the ratio of maximum plasma concentration of unbound test drug (unbound C_{max}) to the IC_{50} value of the drug as an inhibitor of OCT2 activity, can differ markedly depending on whether MPP or metformin is the probe substrate used for determination of IC_{50}.

In light of the growing body of evidence that substrate identity can influence inhibition of drug transport, the FDA recently altered their recommendation, which now suggests that the inhibition constant of a test drug should be determined with a probe substrate that may also be used in later clinical studies (U. S. Food and Drug Administration, 2017), and our results support this view. In the present study we showed that IC_{50}s for inhibition of OCT2-mediated MPP transport are, on average, ~5-fold greater than those for inhibition of metformin transport, thus confirming and extending several previous observations of differential inhibitory sensitivity of these substrates (Belzer et al., 2013; Hacker et al., 2015; Thevenod et al., 2013; Yin et al., 2016). In addition, we showed this to be a common characteristic of OCT2-mediated MPP transport; it proved less sensitive to inhibition than did transport of four additional, structurally diverse

substrates, i.e., cimetidine, TEA, ASP, and NBD-MTMA. Moreover, inhibition of transport of these additional substrates proved to be comparatively similar to inhibition of metformin transport. Taken together, these results support the view that metformin can serve as a representative OCT2 substrate capable of use in both *in vitro* and *in vivo* (i.e., clinical) settings.

The inhibitory profiles were used to generate Bayesian machine learning models that identified structural features most commonly associated with 'active' (i.e., comparatively high affinity) binding to OCT2 (Supp Fig S3). Although these models are generally not appropriate for accurate prediction of clinically relevant IC_{50} values, they proved effective in identifying active inhibitors in a test set of compounds selected from our library of inhibitors. Moreover, they proved equally effective at identifying active inhibitors in a library screened for inhibition of OCT2 transport by a separate research group that used similar, but inevitably different, methods and protocols for one substrate probe, i.e., ASP (Kido et al., 2011). This was a particularly valuable observation in light of growing concern expressed over the substantial variability noted for IC_{50} and kinetic parameters in reviews of studies with multidrug transporters (e.g., (Bentz et al., 2013), including the OCTs (Klaassen and Aleksunes, 2010; Nies et al., 2011b; Wright and Dantzler, 2004), and we have commented on the problems this poses for combining data sets in the literature for the purpose of model development (Ekins et al., 2012). The present observations suggest that, in the future, results be quantitatively compared to values already in the literature, as a means of establishing a validated database to further modeling efforts. Finally, it is worth emphasizing that the anticipated application of our machine learning-derived models is in early preclinical drug discovery where the virtual screening of large libraries of novel structures for their probable interaction with OCT2 can be performed cost-effectively to filter out potentially problematic compounds.

The present results also provide insight into the mechanism of ligand interaction with OCT2. If all substrates and inhibitors 'compete' for a common binding site on or within OCT2, then the IC_{50} for inhibition of transport activity produced by an individual compound should be independent of the identity of the substrate used to assess transport activity (providing the concentration of substrate is well below the K_t for its transport, which was the case for all experiments in the current study) (Segel, 1975). But the routine disparity between IC_{50} values for inhibition of transport of MPP and the other test substrates (Figs. 6, 7 and 8) runs counter to this prediction and necessitates that ligand binding to OCT2 can involve interaction with more than one spatially distinct site. Our earlier observation of competitive, non-competitive and mixed-type inhibition of OCT2-mediated transport (Harper and Wright, 2012) was also consistent with this conclusion. A closer inspection of the current IC_{50} data (Figs. 6, 7 and 8; Fig S2) lends credence to the view that ligand binding to OCT2 is not restricted to interaction with a single, spatially restricted site. Consider the inhibition of OCT2-mediated metformin transport displayed by three structurally dissimilar compounds: fluoxetine, quinidine, and trimethoprim. Whereas their pairwise Tanimoto similarity coefficients are less than 0.5, their measured IC_{50} values were effectively identical (18.6 μM, 18.6 μM and 19.8 μM, respectively; Table 2; Fig. S6). These data suggest that the mechanism of stabilization of ligand binding with a site(s) or surface(s) on OCT2 is unlikely to involve discrete points of interaction between substrate/inhibitor and a single, spatially restricted binding site on the transport protein that favors a set of ligand structural features arranged in the same relative orientation. This is the basis of traditional pharmacophores and may explain the failure of our efforts to generate one or more common feature pharmacophores using the current data set.

The differential interaction of MPP with OCT2 is also evident from the impact on transport of single site mutations to OCT2. In the rabbit ortholog of OCT2, whereas conversion of glutamate to leucine at position 447 (equivalent to E448 in hOCT2) eliminates transport of TEA and cimetidine, it has no effect on transport of MPP (Zhang et al., 2005). The 'outlier' status of MPP may also extend to OCT1: conversion of aspartate to glutamate at position 475 in rat Oct1 (equivalent to D474 in hOCT1) results in a 4 to 14-fold decrease in the apparent K_t values for transport of TEA, N^1-methylnicotinamde and choline, but has no effect on the K_{tapp} for MPP transport (Gorboulev et al., 1999). Both observations are consistent with the view that MPP (and possibly other substrates) may bind to OCTs at multiple sites, one or more of which may exert short distance allosteric effects that contribute to the substrate-dependence of ligand interaction with OCTs. Kinetically, this can present as a 'mixed-type' interaction that involves simultaneous binding of multiple substrate molecules (or substrate and inhibitor molecules) (Harper and Wright, 2012). Moreover, some ligands exert a biphasic inhibition of OCT transport activity that includes both a high affinity (K_i <nM) (partial) inhibition, as well as a low(er) affinity (generally μM to mM) inhibition of transport activity, with the lower affinity interaction being associated with the translocation of substrate (Minuesa et al., 2009; Schophuizen et al., 2013). Lamivudine's inhibition of MPP transport mediated by OCT1, OCT2 and OCT3 displays such biphasic profiles (Minuesa et al., 2009). Interestingly, the high affinity K_i is markedly elevated (from pM to nM) by increasing the concentration of MPP (from nM to μM), which suggests that substrate molecules can occupy multiple sites and that at high (near K_t) concentrations, substrate occupancy of the high affinity (allosteric/inhibitory) site limits inhibitor access. The IC_{50}s we determined did not display biphasic profiles for any of the test inhibitors or substrates, even in those cases (MPP and TEA) where the substrate concentrations were in the

Molecular Pharmacology Fast Forward. Published on June 8, 2018 as DOI: 10.1124/mol.117.111443
This article has not been copyedited and formatted. The final version may differ from this version.

nanomolar range (Fig. 6; Fig. S2). Nevertheless, the growing body of kinetic and structural evidence underscores the mechanistic complexity of ligand interaction with OCTs.

In conclusion, the differential inhibition of OCT2-mediated transport of six structurally diverse substrate molecules produced by a library of 400-480 compounds confirmed previous reports that inhibition of OCT2 activity can be influenced by substrate identity. Transport of MPP was least sensitive to inhibition, and IC_{50} values determined for 20 structurally distinct compounds against transport of MPP, metformin, TEA, NBD-MTMA and ASP were, on average, about 6-fold higher for MPP than the other test substrates. In contrast, IC_{50} values for metformin differed on average only by ~50% from values for the other, non-MPP test substrates. The results support the use of metformin as an OCT2 substrate for assessing clinically relevant interactions with OCT2 (i.e., IC_{50} values), due to its clinical prevalence and utility for both *in vitro* and *in vivo* use. But we also suggest that any of the non-MPP OCT2 substrates studied here can be used to screen NME libraries for the statistical likelihood of adverse drug interactions at the transporter. To that end, well-validated Bayesian models were developed to identify structural elements associated with effective interaction with OCT2.

Molecular Pharmacology Fast Forward. Published on June 8, 2018 as DOI: 10.1124/mol.117.111443
This article has not been copyedited and formatted. The final version may differ from this version.

Acknowledgments

Biovia are kindly acknowledged for providing Discovery Studio to SE.

Authorship Contributions

Participated in research design: PJS, SE, and SHW

Conducted experiments: PJS

Performed data analysis: PJS, KMZ, AMC, SE, and SHW

Wrote or contributed to the writing of the manuscript: PJS, KMZ, AMC, SE, and SHW

Molecular Pharmacology Fast Forward. Published on June 8, 2018 as DOI: 10.1124/mol.117.111443
This article has not been copyedited and formatted. The final version may differ from this version.

References

Aavula BR, Ali MA, Mash EA, Bednarczyk D and Wright SH (2006) Synthesis and fluorescence of n , n , n -trimethyl-2-[methyl(7-nitrobenzo[c][1,2,5]oxadiazol-4-yl)amino]ethanaminium iodide, a pH-insensitive reporter of organic cation transport. *Synthetic Comm* **36**: 701-705.

Belzer M, Morales M, Jagadish B, Mash EA and Wright SH (2013) Substrate-dependent ligand inhibition of the human Organic Cation Transporter, OCT2. *J Pharmacol Exp Ther* **346**: 300-310.

Bentz J, O'Connor MP, Bednarczyk D, Coleman J, Lee C, Palm J, Pak YA, Perloff ES, Reyner E, Balimane P, Brannstrom M, Chu X, Funk C, Guo A, Hanna I, Heredi-Szabo K, Hillgren K, Li L, Hollnack-Pusch E, Jamei M, Lin X, Mason AK, Neuhoff S, Patel A, Podila L, Plise E, Rajaraman G, Salphati L, Sands E, Taub ME, Taur JS, Weitz D, Wortelboer HM, Xia CQ, Xiao G, Yabut J, Yamagata T, Zhang L and Ellens H (2013) Variability in P-glycoprotein inhibitory potency (IC_{50}) using various in vitro experimental systems: implications for universal digoxin drug-drug interaction risk assessment decision criteria. *Drug Metab Dispos* **41**(7): 1347-1366.

Budiman T, Bamberg E, Koepsell H and Nagel G (2000) Mechanism of electrogenic cation transport by the cloned organic cation transporter 2 from rat. *J Biol Chem* **275**: 29413-29420.

Clark AM, Dole K, Coulon-Spektor A, McNutt A, Grass G, Freundlich JS, Reynolds RC and Ekins S (2015) Open source Bayesian models. 1. Application to ADME/tox and drug discovery datasets. *J Chem Inf Model* **55**(6): 1231-1245.

Clark AM and Ekins S (2015) Open source Bayesian models. 2. Mining a "Big Dataset" to create and validate models with ChEMBL. *J Chem Inf Model* **55**(6): 1246-1260.

Ekins S, Polli JE, Swaan PW and Wright SH (2012) Computational modeling to accelerate the identification of substrates and inhibitors for transporters that affect drug disposition. *Clin Pharmacol Ther* **92**(5): 661-665.

Gao F, Johnson DL, Ekins S, Janiszewski J, Kelly KG, Meyer RD and West M (2002) Optimizing higher throughput methods to assess drug-drug interactions for CYP1A2, CYP2C9, CYP2C19, CYP2D6, rCYP2D6, and CYP3A4 in vitro using a single point IC_{50}. *Journal of biomolecular screening* **7**(4): 373-382.

Giacomini KM, Huang SM, Tweedie DJ, Benet LZ, Brouwer KL, Chu X, Dahlin A, Evers R, Fischer V, Hillgren KM, Hoffmaster KA, Ishikawa T, Keppler D, Kim RB, Lee CA, Niemi M, Polli JW, Sugiyama Y, Swaan PW, Ware JA, Wright SH, Wah YS, Zamek-Gliszczynski MJ and Zhang L (2010) Membrane transporters in drug development. *Nature reviews Drug discovery* **9**(3): 215-236.

Gorboulev V, Volk C, Arndt P, Akhoundova A and Koepsell H (1999) Selectivity of the polyspecific cation transporter rOCT1 is changed by mutation of aspartate 475 to glutamate. *MolPharmacol* **56**(6): 1254-1261.

Groves CE, Evans K, Dantzler WH and Wright SH (1994) Peritubular organic cation transport in isolated rabbit proximal tubules. *Am J Physiol* **266**: F450-F458.

Hacker K, Maas R, Kornhuber J, Fromm MF and Zolk O (2015) Substrate-dependent inhibition of the human Organic Cation Transporter OCT2: a comparison of metformin with experimental substrates. *PLoS One* **10**(9): e0136451.

Hagenbuch B (2010) Drug uptake systems in liver and kidney: a historic perspective. *Clin Pharmacol Ther* **87**(1): 39-47.

Harper JN and Wright SH (2012) Multiple mechanisms of ligand interaction with the human organic cation transporter, OCT2. *Am J Physiol Renal Physiol* **304**(1): F56-F67.

Hillgren KM, Keppler D, Zur AA, Giacomini KM, Stieger B, Cass CE, Zhang L and International Transporter C (2013) Emerging transporters of clinical importance: an update from the International Transporter Consortium. *Clin Pharmacol Ther* **94**(1): 52-63.

Holohan PD and Ross CR (1980) Mechanisms of organic cation transport in kidney plasma membrane vesicles: 1. Countertransport studies. *J Pharmacol Exp Ther* **215**: 191-197.

Hu SX, Mazur CA, Feenstra KL, Lorenz JK and Merritt DA (2016) Assessment of inhibition of porcine hepatic cytochrome P450 enzymes by 48 commercial drugs. *Vet J* **211**: 26-31.

Kido Y, Matsson P and Giacomini KM (2011) Profiling of a prescription drug library for potential renal drug-drug interactions mediated by the organic cation transporter 2. *J Med Chem* **54**(13): 4548-4558.

Klaassen CD and Aleksunes LM (2010) Xenobiotic, bile acid, and cholesterol transporters: function and regulation. *PharmacolRev* **62**(1): 1-96.

Liu HC, Goldenberg A, Chen Y, Lun C, Wu W, Bush KT, Balac N, Rodriguez P, Abagyan R and Nigam SK (2016) Molecular properties of drugs interacting with SLC22 transporters

OAT1, OAT3, OCT1, and OCT2: a machine-learning approach. *J Pharmacol Exp Ther* **359**(1): 215-229.

Martinez-Guerrero LJ, Morales MH, Ekins S and Wright SH (2016) Lack of influence of substrate on ligand interaction with human MATE1. *Mol Pharmacol* **90**(3):254-264.

Minuesa G, Volk C, Molina-Arcas M, Gorboulev V, Erkizia I, Arndt P, Clotet B, Pastor-Anglada M, Koepsell H and Martinez-Picado J (2009) Transport of lamivudine [(-)-beta-L-2',3'-dideoxy-3'-thiacytidine] and high-affinity interaction of nucleoside reverse transcriptase inhibitors with human organic cation transporters 1, 2, and 3. *J Pharmacol Exp Ther* **329**(1): 252-261.

Neuhoff S, Ungell AL, Zamora I and Artursson P (2003) pH-dependent bidirectional transport of weakly basic drugs across Caco-2 monolayers: implications for drug-drug interactions. *Pharm Res* **20**(8): 1141-1148.

Nies AT, Hofmann U, Resch C, Schaeffeler E, Rius M and Schwab M (2011a) Proton pump inhibitors inhibit metformin uptake by organic cation transporters (OCTs). *PLoSONE* **6**(7): e22163.

Nies AT, Koepsell H, Damme K and Schwab M (2011b) Organic cation transporters (OCTs, MATEs), in vitro and in vivo evidence for the importance in drug therapy. *Handb Exp Pharmacol* **201**: 105-167.

Pelis RM, Dangprapai Y, Wunz TM and Wright SH (2007) Inorganic mercury interacts with cysteine residues (C451 and C474) of hOCT2 to reduce its transport activity. *Am J Physiol Renal Physiol* **292**(5): F1583-F1591.

Schomig E, Lazar A and Grundemann D (2006) Extraneuronal monoamine transporter and organic cation transporters 1 and 2: a review of transport efficiency. *Handb Exp Pharmacol* **175**: 151-180.

Schophuizen CM, Wilmer MJ, Jansen J, Gustavsson L, Hilgendorf C, Hoenderop JG, van den Heuvel LP and Masereeuw R (2013) Cationic uremic toxins affect human renal proximal tubule cell functioning through interaction with the organic cation transporter. *Pflugers Arch* **465**(12): 1701-1714.

Segel IH (1975) *Enzyme Kinetics*. John Wiley & Sons, New York.

Severance AC, Sandoval PJ and Wright SH (2017) Correlation between apparent substrate affinity and OCT2 transporter turnover. *J Pharmacol Exp Ther*. **362**(3):405-412.

Somogyi A, Stockley C, Keal J, Rolan P and Bochner F (1987) Reduction of metformin renal tubular secretion by cimetidine in man. *Br J Clin Pharmacol* **23**(5): 545-551.

Stage TB, Brosen K and Christensen MM (2015) A comprehensive review of drug-drug interactions with metformin. *Clin Pharmacokinet* **54**(8): 811-824.

Suhre WM, Ekins S, Chang C, Swaan PW and Wright SH (2005) Molecular determinants of substrate/inhibitor binding to the human and rabbit renal organic cation transporters hOCT2 and rbOCT2. *Mol Pharmacol* **67**(4): 1067-1077.

Thevenod F, Ciarimboli G, Leistner M, Wolff NA, Lee WK, Schatz I, Keller T, Al-Monajjed R, Gorboulev V and Koepsell H (2013) Substrate- and cell contact-dependent inhibitor affinity of human organic cation transporter 2: studies with two classical organic cation substrates and the novel substrate Cd^{2+}. *Mol Pharm* **10**(8): 3045-3056.

U.S.Food and Drug A (2012) Guidance for Industry: Drug Interaction Studies - Study Design, Data Analysis, Implications for Dosing, and Labeling Recommendations, (Huang SM and Zhang L eds) pp 1-79.

U.S.Food and Drug Adminstration (2017) Guidance for Industry: In Vitro Metabolism- and Transporter-Mediated Drug-Drug Interaction Studies. pp 1-47.

Volk C, Gorboulev V, Budiman T, Nagel G and Koepsell H (2003) Different affinities of inhibitors to the outwardly and inwardly directed substrate binding site of organic cation transporter 2. *Mol Pharmacol* **64**(5): 1037-1047.

Wright SH and Dantzler WH (2004) Molecular and cellular physiology of renal organic cation and anion transport. *Physiol Rev* **84**(3): 987-1049.

Xu Y, Liu X, Li S, Zhou N, Gong L, Luo C, Luo X, Zheng M, Jiang H and Chen K (2013) Combinatorial pharmacophore modeling of organic cation transporter 2 (OCT2) inhibitors: insights into multiple inhibitory mechanisms. *Mol Pharm* **10**(12): 4611-4619.

Yin J, Duan H and Wang J (2016) Impact of substrate-dependent inhibition on renal organic cation transporters hOCT2 and hMATE1/2-K-mediated drug transport and intracellular accumulation. *J Pharmacol Exp Ther* **359**(3): 401-410.

Zhang X, Shirahatti NV, Mahadevan D and Wright SH (2005) A conserved glutamate residue in transmembrane helix 10 influences substrate specificity of rabbit OCT2 (SLC22A2). *J Biol Chem* **280**(41): 34813-34822.

Zolk O, Solbach TF, Konig J and Fromm MF (2009) Structural determinants of inhibitor interaction with the human organic cation transporter OCT2 (SLC22A2). *Naunyn Schmiedebergs Arch Pharmacol* **379**(4): 337-348.

Molecular Pharmacology Fast Forward. Published on June 8, 2018 as DOI: 10.1124/mol.117.111443
This article has not been copyedited and formatted. The final version may differ from this version.

Footnotes

This work was supported by the National Institute of Diabetes and Digestive and Kidney Diseases [Grant 5R01DK058251]; the National Institutes of Health National Institute of General Medical Sciences [Grant R43GM122196]; the National Heart, Lung, And Blood Institute [Grant 5T32HL07249]; and National Institute of Environmental Health Sciences [Grant 5P30ES006694].

Legends for Figures

Figure 1. Time course of OCT2-mediated uptake of 0.31 μM [^{3}H]MPP, 13.9 μM [^{14}C]metformin, 0.0218 μM [^{3}H]TEA, 0.0134 μM [^{3}H]cimetidine, 3 μM NBD-MTMA and 10 μM ASP. Uptakes are reported as clearance (μl/cm^{2}). These data represent OCT2-mediated transport; i.e., uptake in wild type CHO cells was subtracted from total substrate uptake measured in OCT2-expressing cells Each data point is the mean (±SE) determined in two (MPP, metformin, cimetidine, TEA, and ASP) or three experiments (NBD-MTMA), each using three to five replicate wells. The lines fit to the data for MPP, metformin, TEA, and cimetidine were calculated using an exponential one-phase association function (Prism, GraphPad, San Diego CA); the uptakes of NBD-MTMA and ASP were described by simple linear regression.

Figure 2. The kinetics of OCT2 mediated transport of the six selected substrates. Rates of uptake presented here were corrected for the first-order component of transport (see eq. 1 and Fig. S1). Each data point represents the mean (±SE) rate of mediated (saturable) transport based on 30 second (MPP, metformin, TEA and cimetidine) or two minute (NBD-MTMA and ASP) net accumulation in five to eight replicate wells with eight to twelve different substrate concentrations, determined in three to eight individual experiments. Lines and kinetic parameters were derived from fitting the Michaelis-Menten equation to these data.

Figure 3. The inhibitory effect of 480 test compounds from the National Clinical Collection on the OCT2-mediated transport of ~12 μM [^{14}C]metformin (A) and ~15 nM [^{3}H]MPP (B). The 30 sec accumulation of the two substrates was measured in the presence of a 20 μM concentration of each test agent. The height of the shaded grey region indicates the average (±SE; black lines)

accumulation (expressed relative to uptake measured in the absence of inhibitor, i.e., 'control') determined in two separate experiments, each measured in triplicate and corrected for uptake measured in wild-type CHO cells. The histograms are arranged from no inhibition (left side) to complete inhibition (right side) while the inset in 3B represents the MPP histogram using the rank order derived from the metformin screen in 3A. The horizontal red dashed lines in 3A and 3B indicate 50% inhibition, while the vertical red dashed lines divide the 'active' inhibitors (<50 % of control uptake; to the right) from the 'inactive' inhibitors (>50 % control, to the left). Figure 3C is the pairwise comparison of the inhibitory profiles of MPP and metformin produced by the test compounds from the NCC. The dashed red lines represent 90% of remaining transport; compounds that fall in the upper right quadrant produced little to no inhibition for either substrate. The solid red line is the line of unity and data points that fall on this line represent compounds that inhibited MPP and metformin uptake equally.

Figure 4. The effect of 400-480 compounds from the NCC on the OCT2 mediated transport of NBD-MTMA (A), TEA (B), cimetidine (C) and ASP (D). The 30 sec accumulation of TEA and cimetidine, and the 2 min accumulation of NBD-MTMA and ASP, were measured in the presence of a 20 μM concentration of each test agent. In each histogram the height of the shaded grey region indicates the average (±SE; black lines) accumulation (expressed relative to uptake measured in the absence of inhibitor, i.e., 'control') determined in two separate experiments, each measured in triplicate and corrected for uptake measured in wild-type CHO cells, displayed in order of increasing (left-to-right) inhibition of OCT2-mediated transport (inset histograms are arranged in the same order as metformin inhibitory effectiveness shown in Fig. 3A). Blank spaces that interrupt the inset histograms for cimetidine and ASP represent compounds that were

tested against metformin uptake but were not tested against ASP and cimetidine uptake (80 compounds). The horizontal red dashed lines represents 50% inhibition while the vertical red dashed lines divide the 'active' inhibitors (<50 % of control uptake) from the 'inactive' inhibitors (>50 % control).

Figure 5. Pairwise comparisons of the percentage of remaining OCT2-mediated transport activity (from Figure 4) for NBD-MTMA, TEA, cimetidine, and ASP (y-axes) versus the remaining transport activity for metformin (A,C,E,G) and MPP (B,D,F,H) (x-axes). The lines of unity are represented by solid red lines, and dashed lines represent 90% of remaining transport activity (upper right quadrant is comprised of inhibitors that inhibited transport of both substrates by less than 10%).

Figure 6. Influence of substrate on inhibition of OCT2-mediated transport produced by irinotecan. (A) Effect of increasing irinotecan concentration on OCT2-mediated transport of [^{14}C] metformin (16 μM; solid squares) or [^{3}H]MPP (15 nM; solid circles). Each point is the mean rate of transport measured at each inhibitor concentration (normalized to transport measured in the absence of inhibitor; '% control') measured in two separate experiments (±SE; n=2)), each determined in 4 replicate wells. (B) Data from Fig. 4A, plus the IC_{50} profiles for irinotecan inhibition of [3]TEA (20 nM; open diamonds), NBD-MTMA (3 μM; open circles) and ASP (10 μM; open triangles); error bars removed for clarity.

Figure 7. Pairwise comparisons of IC_{50} values (in μM) for inhibition of OCT2-mediated transport of structurally distinct substrates. (A) Pairwise comparison of IC_{50} values for

inhibition of OCT2-mediated transport of metformin (x-axis) and MPP (y-axis) determined for a subset of 20 compounds selected from the NCC (see Table 2; note the pairwise comparison of IC_{50} values for irinotecan is shown as an open circle). Each IC_{50} is the mean (± SE; n = 2) of values determined in two separate experiments using the experimental design used for the experiments presented in Fig. 6 (also Fig. S2). In this comparison (and the others) the line of unity (equal IC_{50} values for inhibition of both substrates) is represented by the solid red line, and dashed lines represent ratios of IC_{50} values that differ from one another by three-fold. (B and C) Pairwise comparison of measured (x-axes) and predicted IC_{50} values for inhibition of MPP transport (B) or metformin transport (C). Measured values are those shown in Figure 7A (Table 2); predicted values were calculated using the single point method (see Methods). (D) Pairwise comparisons of predicted IC_{50} values for inhibition of metformin transport against those for MPP transport for 162 compounds from the NCC that inhibited transport between 10% and 90%.

Figure 8. Pairwise comparisons of measured IC_{50} values for inhibition of OCT2-mediated transport of either metformin (x-axes, Fig. 8A, B, and C) or MPP (y-axes, Fig. 8 D, E, and F), versus transport of TEA, NBD-MTMA, and ASP (Table 2). Lines of unity (equal IC_{50} values for inhibition of both substrates) are represented by the solid red lines, and dashed lines represent ratios of IC_{50} values that differ from one another by three-fold. Each IC_{50} is the mean (±SE; n=2) of values determined in two separate experiments using the experimental design used for the experiments presented in Fig. 6 (also Fig. S2).

Molecular Pharmacology Fast Forward. Published on June 8, 2018 as DOI: 10.1124/mol.117.111443
This article has not been copyedited and formatted. The final version may differ from this version.

Tables

Table 1

Kinetics of OCT2-Mediated Transport for the Six Test Substrates.

Substrate	K_{tapp} (μM)	SE (±) (μM)	J_{max} (pmol cm^{-2} min^{-1})	SE (±) (pmol cm^{-2} min^{-1})	n
Metformin	285.2	67.5	656.2	42.0	3
MPP	4.6	1.5	17.2	1.5	3
NBD	8.8	2.1	33.2	1.6	3
TEA	57.7	18.3	99.9	10.1	2
Cimetidine	15.1	3.5	18.9	0.7	2
ASP	37.6	21.0	51.1	8.5	8

Molecular Pharmacology Fast Forward. Published on June 8, 2018 as DOI: 10.1124/mol.117.111443
This article has not been copyedited and formatted. The final version may differ from this version.

Table 2

IC_{50} Values for inhibition of OCT2 Mediated Transport of Five Substrates. All uptakes were corrected for the first order (nonsaturable) component of total substrate uptake.

Substrate	Metformin		MPP		TEA		NBD-MTMA		ASP	
Inhibitor	Mean IC_{50} (μM)	Error (±)	Mean IC_{50} (μM)	Error (±)	Mean IC_{50} (μM)	Error (±)	Mean IC_{50} (μM)	Error (±)	Mean IC_{50} (μM)	Error (±)
Amantadine	27.1	0.7	51.0	2.2	32.1	1.5	24.5	1.6	10.1	3.8
Amitriptyline	2.4	0.7	11.3	0.4	5.0	0.6	4.0	0.6	1.8	0.1
Anastrozole	51.1	0.5	327.6	2.6	113.4	9.4	86.0	6.8	39.2	3.0
Atomoxetine	6.6	0.1	20.4	2.3	12.8	2.0	7.6	0.9	3.5	0.0
Atropine	1.3	0.2	12.4	0.8	3.4	0.8	2.3	0.6	1.4	0.1
Benztropine	0.4	0.0	13.4	7.2	1.0	0.1	0.8	0.2	0.3	0.0
Bupropion	8.6	1.8	32.2	5.4	13.4	2.8	10.8	1.0	11.1	1.6
Buspirone	10.2	0.1	68.5	4.4	19.8	1.0	19.6	3.2	8.6	2.6
Fluoxetine	18.6	1.5	56.7	4.5	36.0	5.4	20.1	2.6	16.7	0.8
Imipramine	0.4	0.2	4.9	0.3	1.3	0.3	1.4	0.1	0.5	0.3
Irinotecan	3.3	0.1	15.6	1.4	4.5	0.3	3.2	0.7	1.7	0.0
Mexiletine	21.5	0.6	50.4	5.6	28.5	2.7	30.5	0.7	19.4	4.4
Naloxone	29.5	0.0	235.7	9.2	67.3	2.8	55.1	6.6	20.3	3.7
Pilocarpine	34.5	0.4	109.3	12.2	61.9	0.1	48.2	1.2	55.7	24.1
Quinidine	18.6	1.6	91.1	3.4	23.6	1.0	18.7	1.2	6.4	0.3
Tacrine	0.6	0.0	2.3	0.2	0.9	0.1	1.0	0.3	0.4	0.1
Trimethoprim	19.8	1.8	199.2	54.9	50.2	11.2	43.0	2.7	14.1	1.0
Tripelennamine	2.1	0.2	12.1	2.0	5.0	0.7	5.7	1.0	3.7	0.9
Tropicamide	94.3	2.4	691.5	31.3	205.4	4.6	189.0	1.6	141.4	42.5
Verapamil	10.3	1.0	49.7	3.3	17.8	2.3	9.7	1.9	4.6	1.5

Molecular Pharmacology Fast Forward. Published on June 8, 2018 as DOI: 10.1124/mol.117.111443
This article has not been copyedited and formatted. The final version may differ from this version.

Table 3

Discovery Studio Bayesian model training and test set statistics for each probe substrate and consensus of metformin, NBD-MTMA, TEA, and cimetidine

Training / test	Training / test	ROC LOO	ROC (5 fold)	Sensitivity	Specificity	Concordance
Metformin	Training	0.840	0.802	0.875	0.854	0.858
	Test		0.848	0.643	0.833	0.800
MPP	Training	0.815	0.779	0.919	0.658	0.683
	Test		0.619	0.667	0.514	0.525
NBD-MTMA	Training	0.844	0.806	0.896	0.833	0.845
	Test		0.837	0.857	0.636	0.675
TEA	Training	0.815	0.789	0.895	0.857	0.863
	Test		0.800	0.867	0.754	0.775
Cimetidine	Training	0.827	0.784	0.969	0.758	0.800
	Test		0.806	0.813	0.766	0.775
ASP	Training	0.806	0.768	0.959	0.741	0.791
	Test		0.838	0.842	0.803	0.813
Consensus	Training	0.836	0.798	0.884	0.861	0.865
	Test		0.823	0.857	0.667	0.700

Molecular Pharmacology Fast Forward. Published on June 8, 2018 as DOI: 10.1124/mol.117.111443
This article has not been copyedited and formatted. The final version may differ from this version.

Figures

Figure 1

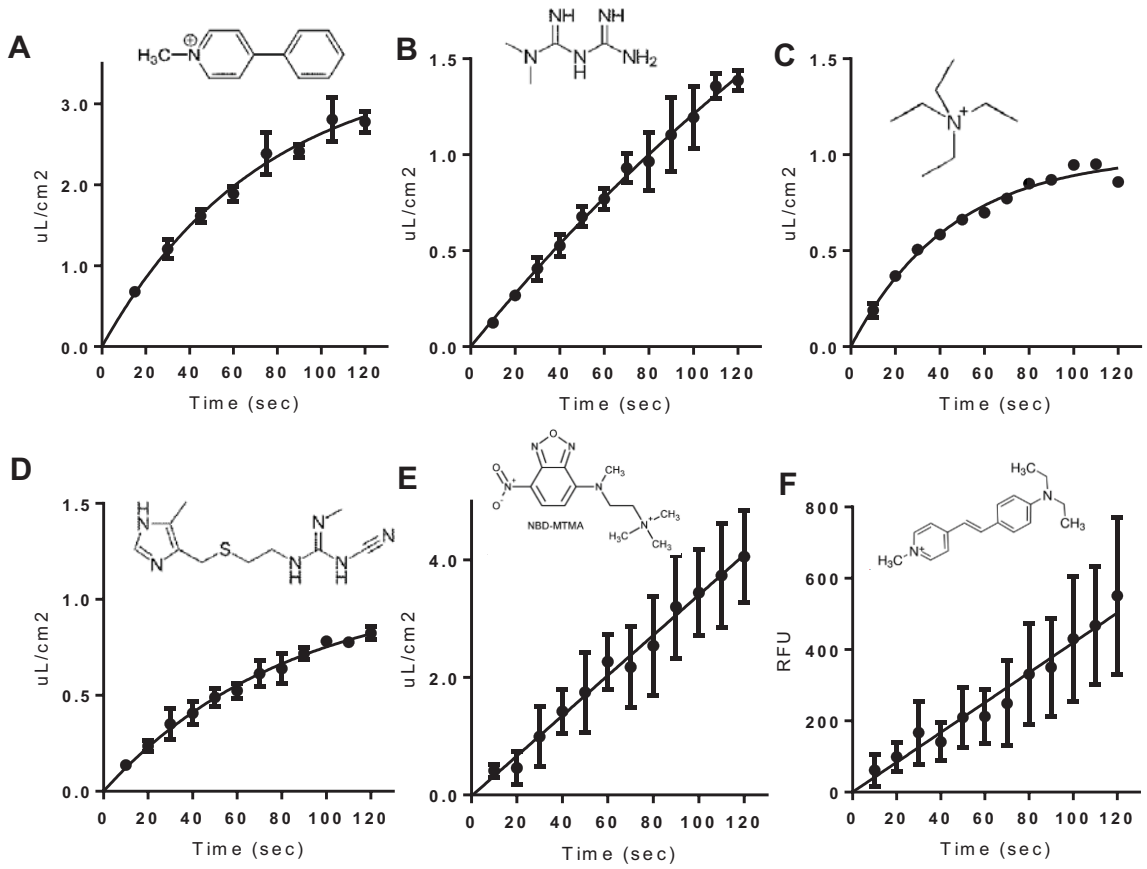

Molecular Pharmacology Fast Forward. Published on June 8, 2018 as DOI: 10.1124/mol.117.111443
This article has not been copyedited and formatted. The final version may differ from this version.

Figure 2

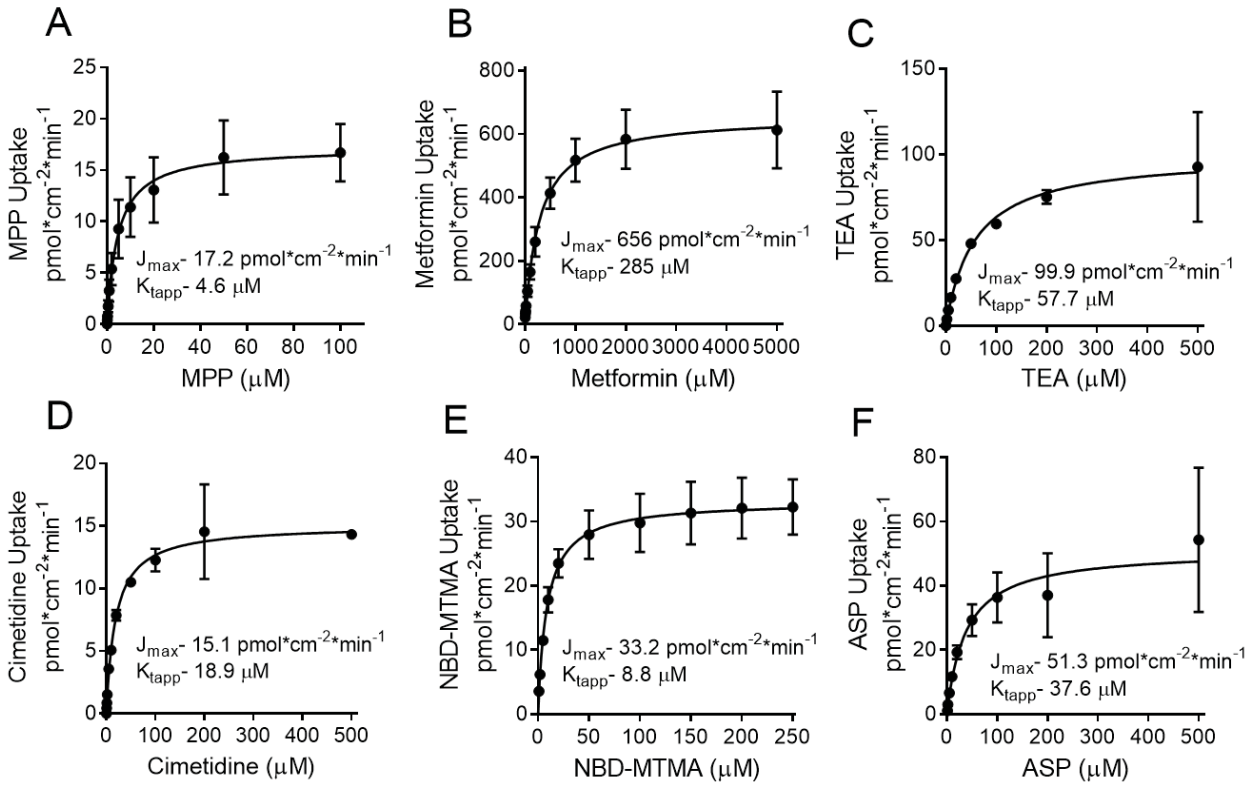

Molecular Pharmacology Fast Forward. Published on June 8, 2018 as DOI: 10.1124/mol.117.111443
This article has not been copyedited and formatted. The final version may differ from this version.

Figure 3

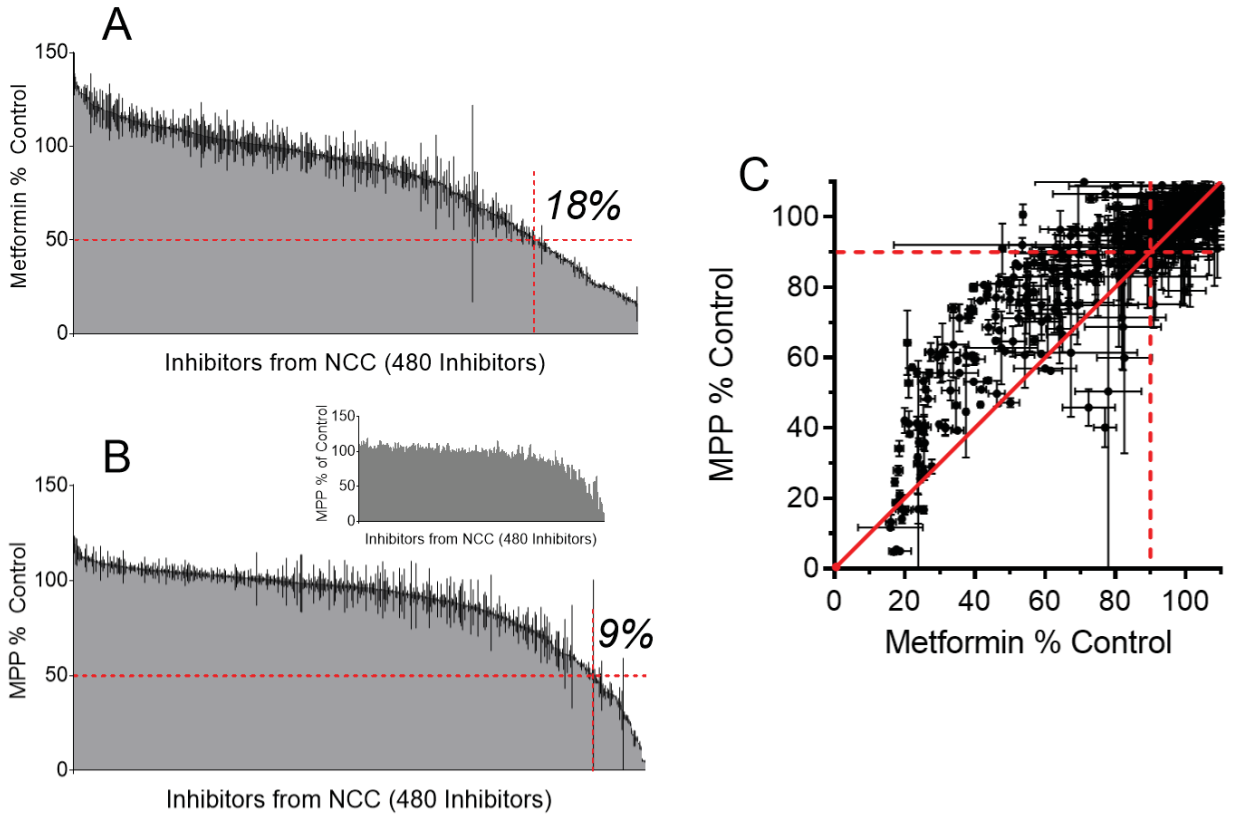

Molecular Pharmacology Fast Forward. Published on June 8, 2018 as DOI: 10.1124/mol.117.111443
This article has not been copyedited and formatted. The final version may differ from this version.

Figure 4

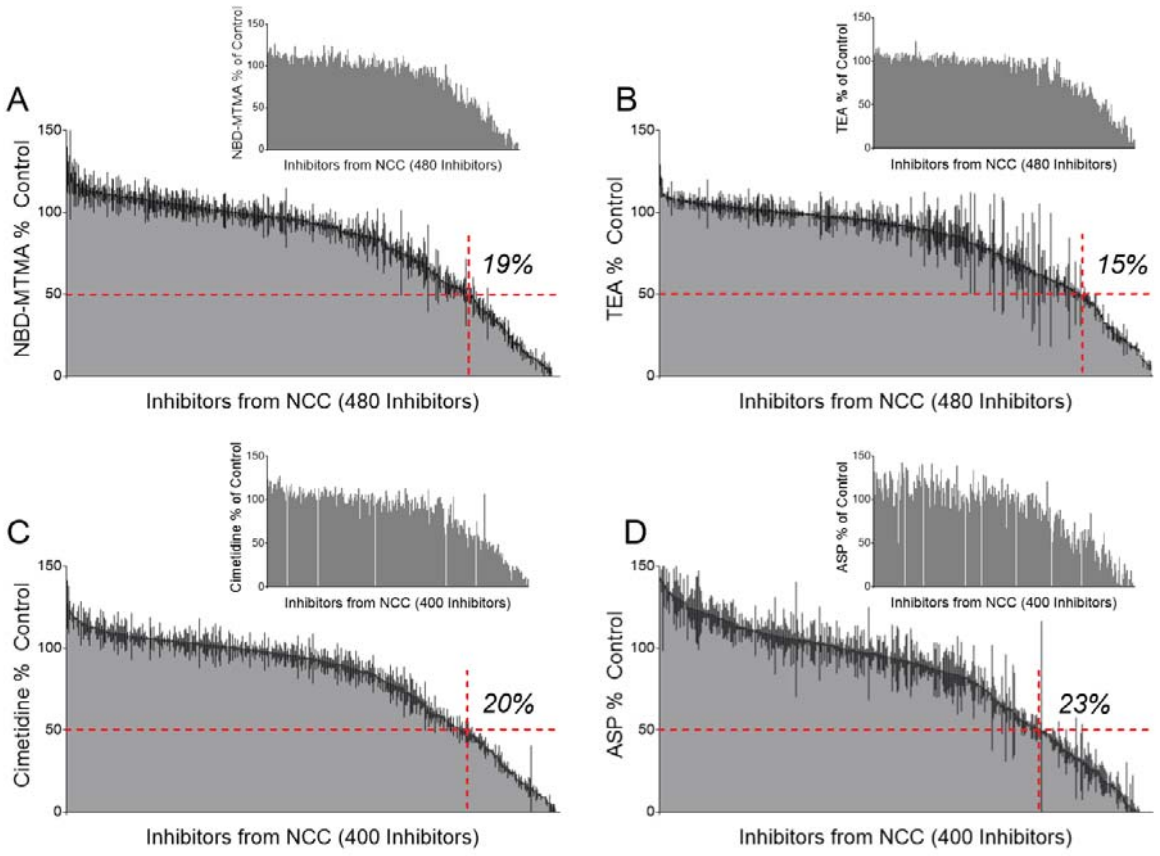

Molecular Pharmacology Fast Forward. Published on June 8, 2018 as DOI: 10.1124/mol.117.111443
This article has not been copyedited and formatted. The final version may differ from this version.

Figure 5

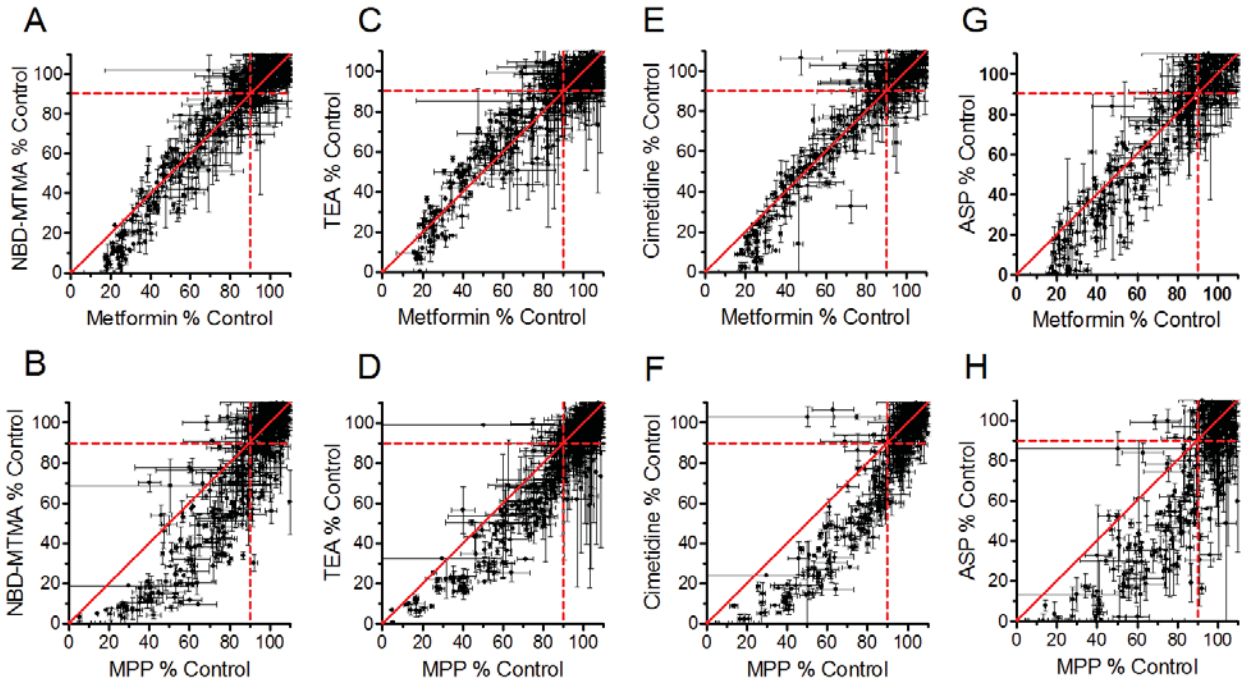

Molecular Pharmacology Fast Forward. Published on June 8, 2018 as DOI: 10.1124/mol.117.111443
This article has not been copyedited and formatted. The final version may differ from this version.

Figure 6

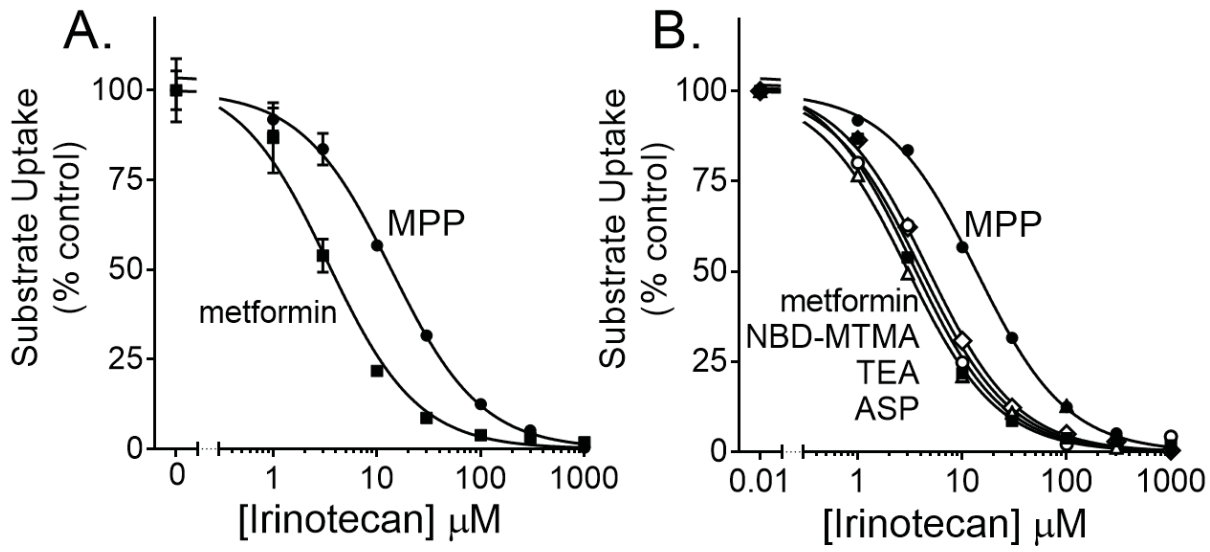

Molecular Pharmacology Fast Forward. Published on June 8, 2018 as DOI: 10.1124/mol.117.111443
This article has not been copyedited and formatted. The final version may differ from this version.

Figure 7

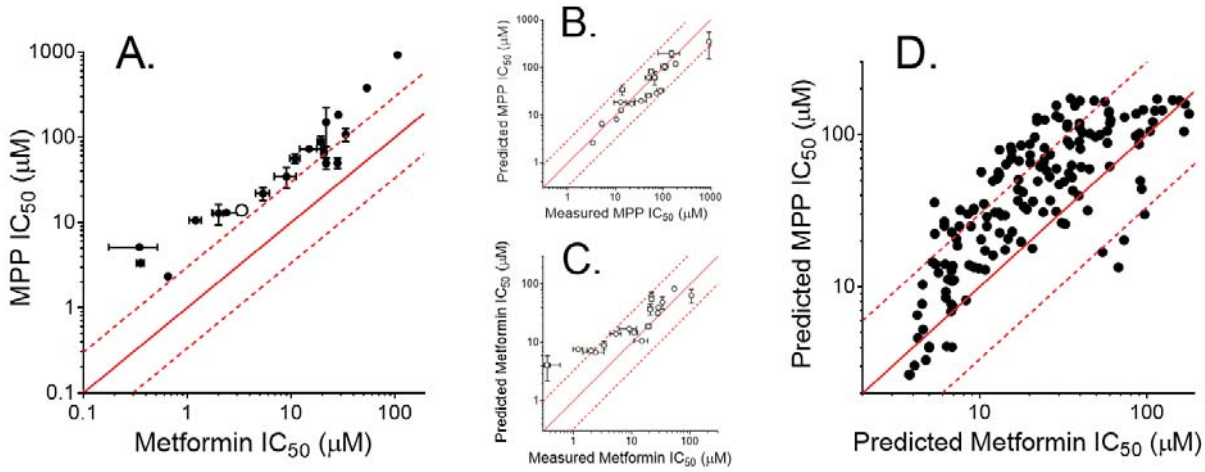

Molecular Pharmacology Fast Forward. Published on June 8, 2018 as DOI: 10.1124/mol.117.111443
This article has not been copyedited and formatted. The final version may differ from this version.

Figure 8